Solvent Extraction and Ion Exchange

ISSN: 0736-6299 (Print) 1532-2262 (Online) Journal homepage: http://www.tandfonline.com/loi/lsei20

Liquid–Liquid Mixing Studies in Annular Centrifugal Contactors Comparing Stationary Mixing Vane Options

Kent E. Wardle

To cite this article: Kent E. Wardle (2015): Liquid–Liquid Mixing Studies in Annular Centrifugal Contactors Comparing Stationary Mixing Vane Options, Solvent Extraction and Ion Exchange, DOI: 10.1080/07366299.2015.1082835

To link to this article: http://dx.doi.org/10.1080/07366299.2015.1082835

Accepted online: 11 Sep 2015.Published online: 11 Sep 2015.

Solvent Extraction and Ion Exchange, 00: 1–20, 2015
Published with license by Taylor & Francis
ISSN: 0736-6299 print / 1532-2262 online
DOI: 10.1080/07366299.2015.1082835

LIQUID–LIQUID MIXING STUDIES IN ANNULAR CENTRIFUGAL CONTACTORS COMPARING STATIONARY MIXING VANE OPTIONS

Kent E. Wardle

Chemical Sciences and Engineering Division, Argonne National Laboratory, Argonne, IL, USA

Comparative studies of multiphase operation of an annular centrifugal contactor show the impact of housing stationary mixing vane configuration. A number of experimental results for several different mixing vane options are reported for operation of a 12.5 cm engineering-scale contactor unit. Fewer straight vanes give greater mixing-zone hold-up compared to curved vanes. Quantitative comparison of droplet size distribution also showed a significant decrease in mean diameter for four straight vanes versus eight curved vanes. This set of measurements gives a compelling case for careful consideration of mixing vane geometry when evaluating hydraulic operation and extraction process efficiency of annular centrifugal contactors.

Keywords: ***Annular centrifugal contactors, liquid-liquid extraction, nuclear fuel cycle, nuclear separations***

INTRODUCTION

While annular centrifugal contactors have been in use for solvent extraction processes since their development in the 1970s as part of nuclear fuel cycle research and development at U.S. Department of Energy facilities,[1,2] aside from a few minor variations and fabrication considerations, their basic design has not varied appreciably over that period. Though such contactors may appear complex at first look, when their operation is better understood it is found they rely on very basic principles and as a unit contain only a single moving part—the rotor. Figure 1 shows a sketch of a generalized annular centrifugal contactor.

The flow within a centrifugal contactor is as follows: two immiscible liquid phases having differing densities enter through separate inlets into the narrow annular gap between the stationary outer housing and rotating outer surface of the spinning rotor. Mixing of the two liquids occurs in this annular space. The extent of mixing (i.e., droplet size, interfacial area), the overall volume hold-up in this annular mixing region, and the space below the

Address correspondence to Kent E. Wardle, Chemical Sciences and Engineering Division, Argonne National Laboratory, Argonne, IL 60439. E-mail: kwardle@anl.gov

Color versions of one or more of the figures in the article can be found online at www.tandfonline.com/lsei.

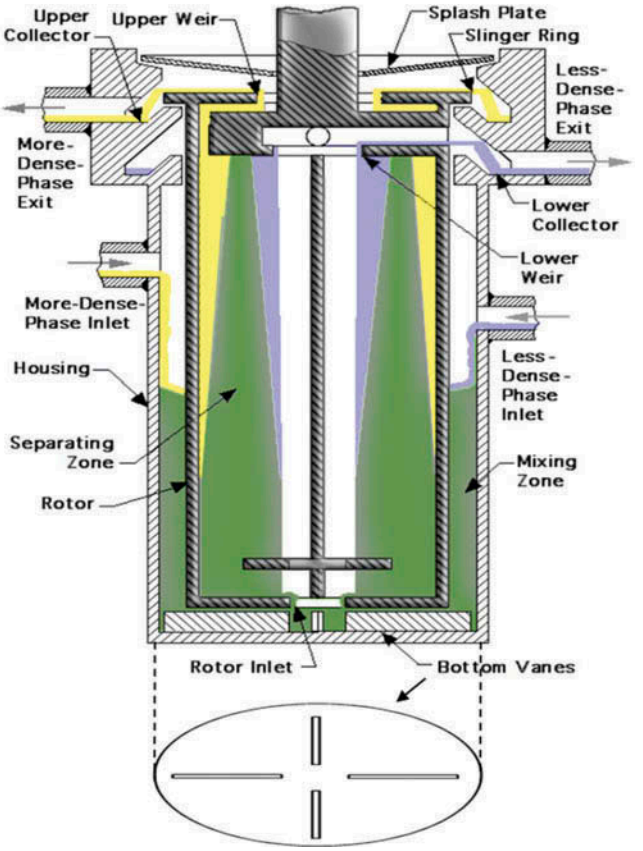

Figure 1 Sketch of the layout of a generalized annular centrifugal contactor showing an example profile of the stationary housing bottom plate with four straight vanes.

rotor for the given flow conditions (i.e., residence time) are the prime factors in determining the extent of extraction of the desired species for the targeted chemistry. Stationary vanes attached to the housing and below the rotor serve to break the rotation of the fluid dispersion (avoiding a vortex) and direct it toward the central opening at the bottom of the rotor. Inside the rotor, the force created by the high-speed rotation accelerates the separation of the phases to several hundred times that achieved in gravity conditions. As the fluids flow upward in the rotor, they become fully separated and are split off by flowing over their respective weirs, exiting the rotor, and each being collected in separate stationary troughs that surround the rotor. Each phase exits the stage and flows by gravity out to a successive stage or collection vessel. In this way, the contactor performs all the actions of a mixer, centrifuge, and pump using a single moving part and with a compact footprint.

A critical performance measure for an extraction device is its stage mass transfer efficiency which is defined as the fractional approach to thermodynamic equilibrium:[3]

$$E_{MD} = \frac{C_{D,in} - C_{D,out}}{C_{D,in} - C_{D,equil}} \tag{1}$$

where E_{MD} is the Murphree efficiency based on the concentration of the dispersed phase *CD*. For a given extraction chemistry and complete physical separation of the phases at each stage (no back-mixing), mass transfer efficiency can be increased at the equipment level in two main ways: decreasing the dispersed phase droplet size (increasing the liquid–liquid interfacial area) and/or increasing the contact time during which mass transfer occurs. While a number of design variables that influence a contactor's stage extraction efficiency have been identified, configuration options for an existing piece of equipment are typically limited to changes in the radius of the heavy phase (upper) weir and the geometry of the housing vanes. From the operational perspective, additional control of performance can be achieved through variation of the rotor speed, feed rates, and feed organic-to-aqueous flow ratio (O/A). While there are some tools to aid in selection of the heavy phase weir size,[4] little guidance is available on selection of housing vane geometry to optimize unit operation for desired flow conditions—which are themselves typically pre-determined by the desired chemical process outcomes rather than by engineering considerations of the conditions for best hydraulic operation of the device as long as the hydraulic operation is stable and acceptable.

Previous two-phase (liquid/gas) experimental[5] and computational studies[6] have explored the impact of the configuration of the stationary housing vanes on the height of the liquid in the annular mixing zone. From this, an expected mixing behavior for different vane configurations can be inferred with vanes (and operational conditions) that produce a higher liquid height yielding a smaller average dispersed phase droplet size and a proportionally longer residence time due to increased hold-up volume. Some limited multiphase computational fluid dynamics (CFD) studies have also been recently reported which again provide a relative comparison of the impact of different housing vanes on mixing.[7] From these studies it has been proposed that the use of fewer, straight vanes (e.g., four straight vanes) gives a higher liquid height (larger mixing zone hold-up), longer residence time, and smaller average droplet size. Birdwell and Anderson[8] performed cesium extraction studies comparing process separation efficiency for straight vanes versus curved vanes in a 5 cm contactor and found noticeable improvement in the straight vane configuration as compared to curved one.

This current work aims to explore the hydraulic operation of annular centrifugal contactors with regard to mixing vane type by building upon the thorough single-liquid studies reported previously.[5] Such a comparison necessitates measurements of mixing zone hold-up under two-phase conditions. Direct measurements of droplet size and distribution are also necessary to make a quantitative comparison. Both of these present significant experimental challenges in general, and particularly when working with centrifugal contactors.

Centrifugal contactor mixing zone hold-up is difficult to quantify as it is not possible to directly measure *in situ*, and it is generally a challenge to differentiate liquid within the rotor from that in the annulus when taking measurements of total stage hold-up (such as using an overall mass balance). Schuur and colleagues[9,10] have presented results for absolute single stage hold-up in the mixing zone using measurements of the overall phase volume ratio and overall hold-up. Given the multiple uncertainties built into the estimations, the error bounds on such values are likely significant (though unreported) and it is not clear if reliable conclusions can be made from trends in the data. Further, the data are for very low flow rates ($\leq$ 100 mL/min) that is less than 5% of the maximum throughput of a device of the size used (5 cm rotor). As the authors of the study note, under these conditions the liquid level in the annulus is barely above the bottom edge of the rotor. Mixing performance would

be expected to be extremely poor and inconsistent in such conditions and thus, these results are difficult to extrapolate with utility to more typical operating conditions or larger-scale contactor units. The work of Kadam et al.[11] purports to provide "dispersed phase hold-up" measurements; however, what is reported is only the dispersed phase volume fraction in the mixing region and not the actual hold-up volume.

It is also possible to estimate the phase volumes in the mixing region by stopping the feed pumps and draining the mixing zone with the rotor still running. This method introduces some uncertainty as there may be inconsistent drainage from the inlet lines and/or "loss" of fluid into the rotor as it continues pumping from the mixing zone. Given these challenges, a reliable method for measurement of mixing zone hold-up is still unavailable. While not a complete solution, a method and supporting data have been developed and are reported elsewhere[12] for quantifying the relative difference in hold-up volume between different housing vane types at the same operating conditions. General trends follow the liquid height observations reported in this work.

Measurement of droplet size is also quite challenging given the small droplet sizes found in these contactors ($\leq$ 100 μm), their fast motion under operating conditions, the opacity of the dispersion given the typically high dispersed fraction (up to $\sim$50%) and the entrainment of air bubbles in the flow, and the restricted flow space of the mixing zone. A number of methods for *in situ* measurement are available including both image processing and laser-based techniques, though it has been shown that large discrepancies can exist between the data measured using the various tools, and direct imaging and image processing is still considered the most reliable.[13] In addition, the use of an intrusive probe is questionable in centrifugal contactors given the limited flow area of the mixing zone. Schuur et al. give data obtained from a focused beam reflective measurement (FBRM) probe positioned between housing vanes under the rotor. The exact location of the measurement relative to the rotor and vane surfaces is not clear though it is stated that the probe fills the gap between the rotor and housing bottom—this significant obstruction would certainly affect the flow in the measurement region to some degree. Further based on similar measurements reported elsewhere[14] and in the current work, the values they obtained are significantly smaller than would be expected for the liquid phases employed and the very poor mixing conditions of the device at the operating conditions employed as noted previously. The apparent under-prediction of the droplet size in these measurements is consistent with the comparison of Maaß et al.[13] in which FBRM was found to give results an order of magnitude smaller than those from direct imaging using an endoscope probe.

Recently, Wyatt et al.[14] performed droplet size distribution measurements using non-intrusive direct image processing for a lab-scale 5 cm rotor centrifugal contactor with a curved vane configuration looking at the impact of rotor speed and O/A ratio for oil dispersed conditions in a water/PDMS system at a constant total throughput of 300 mL/min. The measurement location for almost all conditions was on the side of the housing at the mid-height of the annular liquid level—thus the absolute location varied slightly with liquid level changes between measurements, making interpretation of the data at different conditions somewhat problematic. Additionally, only a configuration with eight curved housing vanes was considered with an overall flow rate that was quite low making annular hold-up and mixing performance rather poor. The present study aims to provide quantitative comparisons of hold-up and droplet size under more typical operating conditions using fluid phases of direct relevance to nuclear separations applications.

Sathe and co-workers also report measurements of droplet size distribution[15] using laser induced fluorescence and image processing. However, this study was conducted for a

simple annular mixer that was liquid-full (no air) and under moderate mixing conditions. Thus, the average droplet sizes reported are quite large ($\geq$ 1 mm) and the results are not useful for application to more typical configurations and conditions or for the present purpose of evaluating differences in centrifugal contactor design (i.e., mixing vane geometry).

We report here a number of measurements aimed at elucidating differences in hydraulic performance for different mixing vane configurations including comparisons of mixing zone hold-up, phase distribution, and droplet size.

EXPERIMENTAL SETUP

Liquid-liquid mixing tests were done in a CINC Industries V05 model centrifugal contactor having a 12.5 cm (5 in) diameter rotor. The unit has unique customizations to enable optical measurements of the mixing zone both in the annular region and the housing vane region. Some companion measurements in the smaller CINC V02 lab-scale contactor are reported elsewhere.[16]

The CINC V05 contactor has a lower housing (housing body below the collector ring portion – see Fig. 1) made of machined acrylic. The main body of the rotor has also been constructed of acrylic though not primarily for optical access, but rather to make it electrically insulating to facilitate measurements in the annular space using electrical resistance tomography (ERT). ERT is a method by which successive pairwise measurements of conductivity on an array of electrodes are tomographically reconstructed to obtain a cross-sectional phase distribution.[17] The housing of the contactor has been fitted with 8 vertical arrays of 16 rectangular electrodes plus an upper ground for each array (total 136). These 8 arrays of electrodes are equally spaced around the circumference of the rotor with the bottommost located just above the rotor bottom. Additionally, a circular array of 32 square electrodes is also included in the instrumented housing and is positioned just below the bottom edge of the rotor near the tops of the mixing vanes. Only selected results from the circular array are reported here. All electrodes are inset into the inner housing wall so as to minimize any impact on the flow in the annular space. The electrodes are connected to an 8-plane (8 x 16 electrode channels) p2+ ERT System from Industrial Tomography Systems to acquire both point voltage measurements and tomographic reconstructions for measurement of liquid phase fractions under multiphase operation with a single liquid phase (and air) or two liquid phases. A picture of the instrumented contactor during operation is shown in Fig. 2.

The contactor unit is also equipped with a changeable bottom plate with attached vanes of various configurations including CINC's "standard" 8 curved vanes and straight vane plates with 4, 6, and 8 vanes. Throughout this paper, these vane configurations will be denoted as CV, 4V, 6V, and 8V. The vane plates are made of polished acrylic to provide good optical clarity for imaging of the dispersion from the bottom side of the housing. The curved vane geometry of the V05 has uniform full-height vanes which differs from that for the V02 model contactor which has a non-uniform, two-tiered vane height as noted elsewhere.[6] For the V05 contactor, each of the four vane types also had a radial gap of approximately 0.25 in (0.635 cm) between the outer edge of the vane and the inner wall of the housing. For these measurements the aqueous weir diameter for the V05 contactor was 2.55 in (6.45 cm).

The V05 contactor unit was set up in a flow loop that could be configured either for once through operation or continuous recycle. Feed and return tanks for both solutions were maintained on balances monitored by a custom LabView interface to provide means for

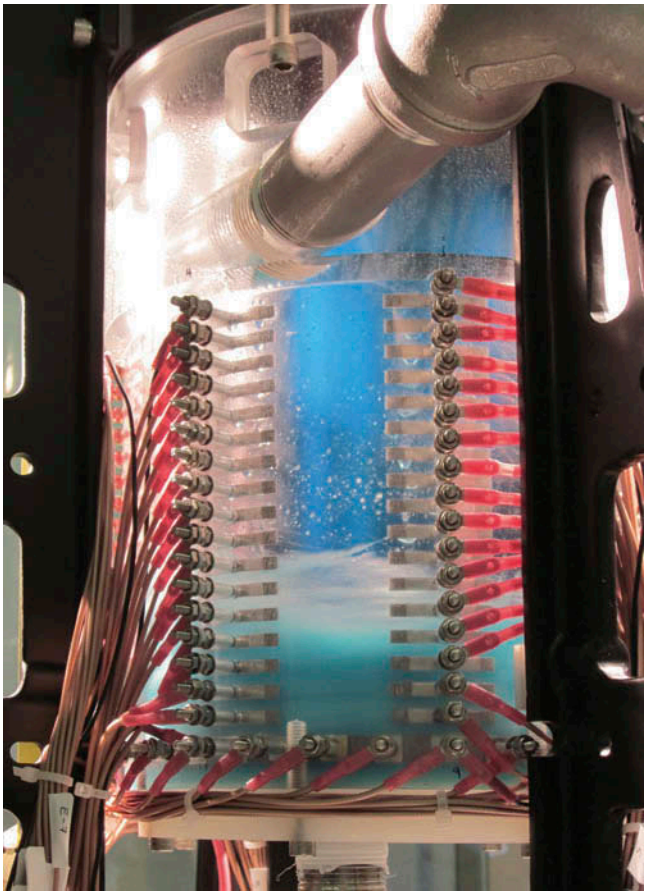

Figure 2 Snapshot of electrode instrumented CINC V05 contactor during liquid-liquid operation. The aqueous phase is dyed blue. The liquid inside the rotor can be seen in the interior of the contactor above the lighter blue mixed phases in the foreground.

calibrating flow rates and monitoring steady-state conditions. Flow pumping was provided by Micropump GL series gear pumps.

Two different liquid-liquid pairs have been used for the experiments reported here. Tests were first done in each of the contactors using a liquid-liquid phase pair consisting of:

Aqueous Phase: 37.5 wt% aluminum nitrate (1 M)(Fisher Chemical, CAS 7784-27-2) in 8 wt% nitric acid (1 M)(Fisher Chemical, CAS 7697-37-2), density = 1.172 g/cm^3.

Organic Phase: 40 vol% tributyl phosphate (TBP)(Sigma Aldrich, lab grade, CAS 126-73-8) in dodecane (Acros Organics, technical grade mixture of isomers, CAS 93685-81-5), density = 0.855 g/cm^3.

The aqueous phase was dyed with methylene blue to aid in visual phase discrimination. The addition of aluminum nitrate to the aqueous phase and use of 40 vol% TBP was intended

to produce a measurable electrical conductivity in the organic phase through "salting out" additional nitrate ions to enable electrical resistance tomography (ERT) measurements under both organic continuous and aqueous continuous conditions in the modified V05 contactor. Indeed, the measured conductivities of the aqueous and organic phases were 169 mS/cm and 7.6 μS/cm, respectively. In the p2+ device, a specified electrical current is "injected" or induced between each pair of adjacent electrodes in the measurement array, and the resulting voltage is measured at the remaining electrodes meaning that such high conductivity solutions are not usable with this device due to a limitation in the maximum injection current setting (75 mA). In such cases, it was found that the relatively high conductivity of the aqueous phase swamped the p2+ system when configured with settings optimized for the organic phase and thus, only aqueous continuous measurements were possible, and even then the highest injection current setting was required. High-speed imaging of the annular mixing zone was also performed for both contactor sizes with this phase pair. Unless otherwise specified, the results presented in this paper are from this phase pair.

Given the limitations found in ERT tests using the previous liquid–liquid phase pair, the two-phase system of 30% TBP in dodecane and 0.01 M nitric acid was also used for ERT and high-speed imaging for droplet size distribution measurements. A small amount of organic soluble Nile Red fluorescent dye was added to aid in visual phase discrimination, particularly for droplet imaging and sizing. Data were acquired for aqueous continuous conditions at an O/A of 0.333 and a total throughput of 10 L/min at 1800 RPM.

High speed imaging of the mixing zone as seen through the side of the transparent housing of each contactor was also performed to provide additional insight into single- and two-fluid operation, and in the case of the 12.5 cm unit, to verify liquid height measurements taken from the linear ERT arrays. The high-speed camera was a Redlake (IDT) MotionPro X5plus model capable of 500 frame/second imaging at a resolution of 2352 x 1728 (4 megapixels) and increased speed at reduced resolution. Typical measurements consisted of 1000 frames taken at 500 frames/second (duration of 2.0 s of flow) which were then averaged to give the results reported here. Longer videos at a much reduced framerate were also taken to observe the dynamics of long transients ($\sim$20 s) such as during start-up or shut-down.

Direct *in situ* imaging of the liquid–liquid dispersion for obtaining droplet size distributions was done using a setup consisting of a high-power, short-pulse strobe light coupled with a high-resolution digital single lens reflex (DSLR) camera, and a long-range telecentric microscope lens. The strobe light was the SPOT 500 ns flash from Prism Science Works which was triggered directly from the camera (16.2 Mpx, Nikon D7000). This combination of a strobe and camera allows for an effective 500 ns camera exposure giving high resolution stills at a small fraction of the expense required for a comparable short exposure high-speed camera with requisite pulsed laser lighting as commonly used for such applications. A precision telecentric lens with excellent light economy is also essential to obtaining sharp images for droplet sizing. Towards this end we employed the Infinity K1 CentriMax lens with an MX-6 objective attachment and two NTX-2x adapter tubes in series. This setup allows for imaging over a field of view (FOV) of approximately 1.5 mm x 1 mm. Imaging of the dispersion was performed through the housing bottom vane plates with, based on advice from the lens manufacturer, a microscope cover glass liquid-adhered to the outer acrylic surface, vastly improving the clarity of the images. Given the limited access under the contactor bottom, a right angle mirror attachment was used. Having the mirror thus

attached to the lens eliminated issues with independent positioning of a separate mirror. Image processing was done in a user-driven, semi-automated manner using the ImageJ software package.

RESULTS AND DISCUSSION

The experimental results for each of the different mixing zone configurations are presented here. Only studies for liquid–liquid operation are included here though additional work in quantification of relative hold-up and annular liquid height for single-phase operation are reported elsewhere.[12] Measurements are reported for annular liquid height, flow under the rotor in the mixing vane region, and droplet size distribution measurements at the bottom of the housing.

Annular Liquid Height

The height of liquid in the annulus was observed by high-speed imaging of the flow using the aluminum nitrate/nitric acid and TBP/dodecane system. Figure 3 shows time averages of the high-speed images as viewed from the contactor side for three flow rates in liquid–liquid operation at an O/A flow ratio of 1:1 in the 12.5 cm contactor (CINC V05). Under these conditions the flow is organic continuous as confirmed by electrical conductivity measurements. The published maximum throughput of this unit is approximately 20 L/min, and the flow rates tested were 5, 10, and 15 L/min—or 25%, 50%, and 75% of total throughput.

A test for the highest flow rate in the 4V geometry was not performed as the liquid volume in the mixing zone was above the height of the inlets under these conditions—the inlet height is just above the top of the image. The same trends in liquid height as seen in the single liquid (water) tests reported in the previous section are evident here: 4V > 6V > 8V > CV. In the liquid–liquid case, the differences in liquid height are enhanced over the water-only case as the mixture viscosity for the liquid-liquid dispersion is greater than that of water, leading to higher liquid height in all cases. Banding of the aqueous phase is also apparent in individual snapshots, but is somewhat washed out by the time-averaging. This evidences the dynamic axial motion (i.e., liquid height oscillations) and variability of the bands, particularly for larger liquid height cases such as in the 4V and 6V geometries. Interestingly, the liquid height for 6V at 5 LPM is roughly equal to that for 8V at 10 LPM and CV at 15 LPM such that the images on the top-left to bottom-right diagonals in the image matrix have roughly equivalent liquid height.

The variation in liquid height for different O/A ratios for the four vane types (at 10 LPM total flow) is shown in Fig. 4.

Inflow of the organic phase—which enters just above the upper right edge of the image and flows downward from right to left—can be seen in some cases (e.g., O/A = 1/3, 6V case). With increasing organic flow fraction there is an increase in liquid height and also greater air entrainment as evidenced by increased light scattering. The height variation across the vane types is most pronounced at O/A = 1. This may be due to the mixture viscosity having a maximum in the range of 1:1 phase ratio.[18]

Similar trends are seen for companion liquid–liquid measurements in the lab-scale V02 contactor reported separately[16] though there are some minor differences due to changes in the vane geometry between the two contactor sizes. It was found that in the V02 CV configuration the relative liquid height was higher than 8V while for the

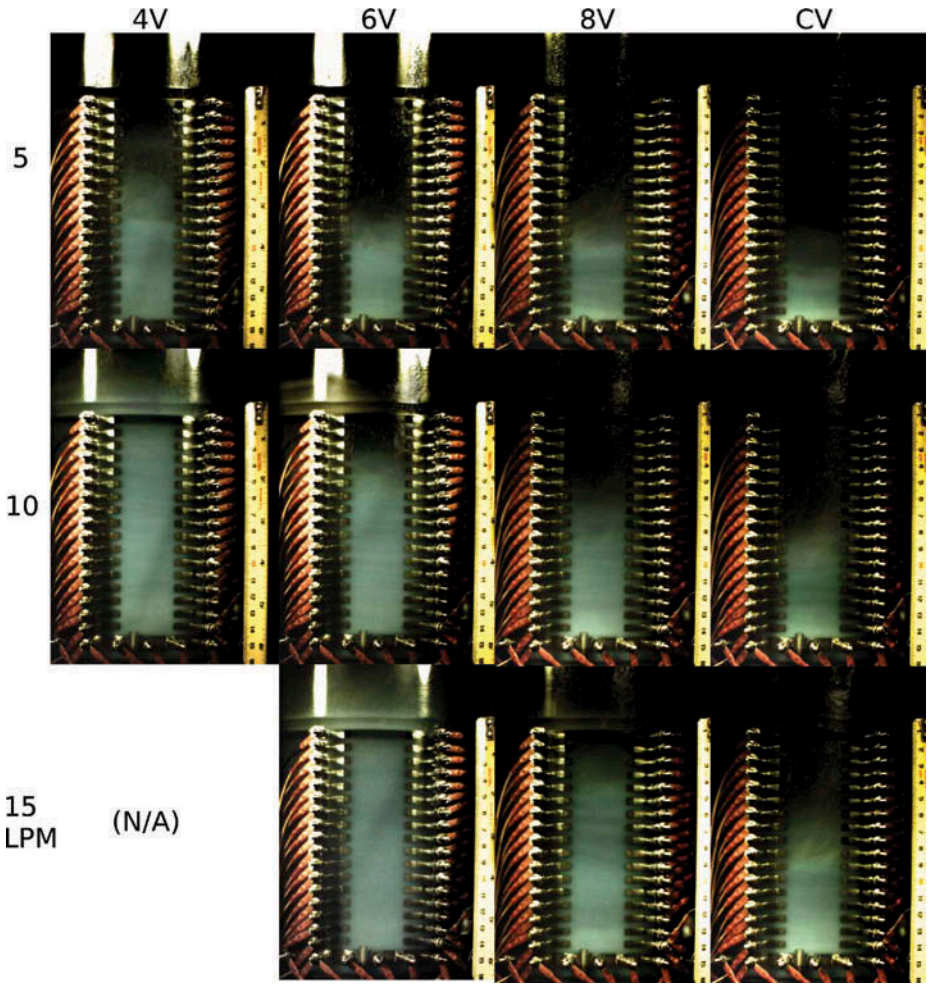

Figure 3 Time-averaged images of annular liquid hold-up at O/A = 1 for four different vane types (columns) and three different flow rates (rows) as viewed from the housing side just downstream (in the rotational direction) of the light phase inlet. All cases are at a rotor speed of 1800 RPM.

V05 contactor this was not the case. The addition of a radial vane-wall gap for the vanes in the larger contactor resulted in a slightly higher liquid height in all straight vane cases in the V05 relative to the V02. Additionally, the differences noted above in the curved vanes between the two cases—namely, the lower vane height on the outer portion of the vane—resulted in a slightly higher liquid height (in relative terms) in the V02 as compared to the V05 due to an apparent decrease in the effective pumping efficiency of the vanes.

It is clear that even minor variations in vane geometry can have a measurable effect on liquid height. What is yet to be quantified is the magnitude of this effect in terms of its potential impact on extraction efficiency. One way to quantify these differences is through *in-situ* measurements of droplet size as reported later.

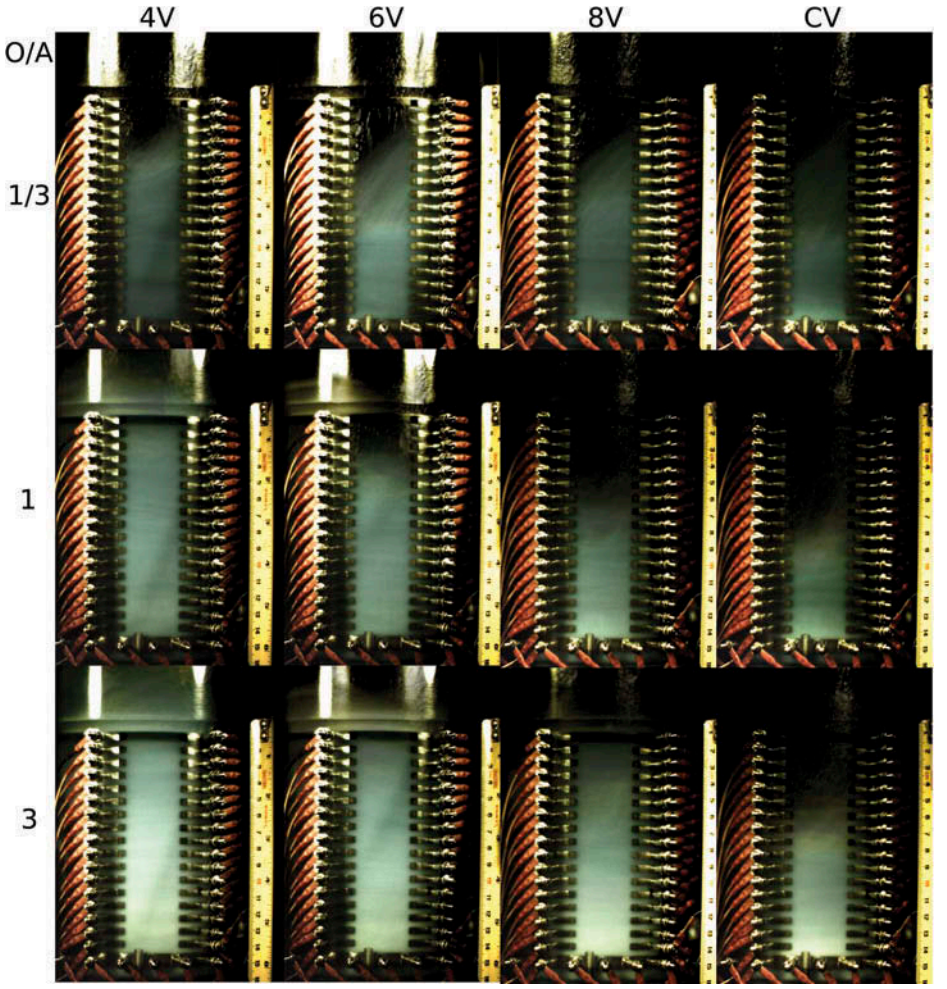

Figure 4 Time-averaged images of annular liquid hold-up at 10 LPM for four different vane types (columns) and three different O/A flow ratios (rows). All cases are at a rotor speed of 1800 RPM.

Flow in Mixing Vane Region

High-Speed Imaging. The flow underneath the rotor of the 12.5 cm contactor for each of the four different vane types is shown in Fig. 5 with the bottom row showing instantaneous snapshots and the top row time-averaged images (converted to grayscale). Note that all cases are at 10 LPM, O/A = 1, and 1800 RPM except the CV case which is at 1200 RPM. Images were taken at 500 fps.

Under these conditions, the dyed aqueous phase is dispersed and darker regions should thus be aqueous-rich. At first inspection, it was unexpected that the center of each rotating region between vanes would have a higher concentration of the more heavy phase. However, recent CFD simulations using coupled dispersed/segregated phase models[19] have confirmed that these dark regions are indeed aqueous-rich. While it seems counterintuitive that the heavy phase would go towards the center of rotation rather than outward, as the dispersed phase, the droplets also have the tendency to go towards regions of lower flow

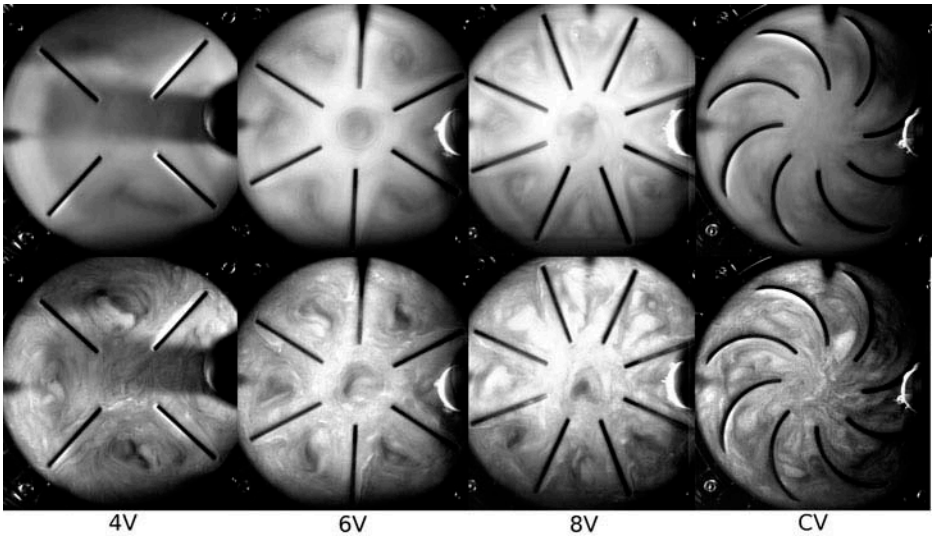

Figure 5 Instantaneous snapshots (bottom) and time-average images (top) for flow at 10 LPM and O/A = 1 in the mixing vane region for four different vane types. The rotor speed was 1800 RPM in all cases except CV which was at 1200 RPM. Rotor rotation is in a clockwise direction.

velocity, a tendency which appears to dominate over density variations in this case. It can be seen that for the 6V and 8V cases, these regions are most pronounced and an additional counter-rotating vortex is observed in the center near the rotor axis as noted in early CFD simulations.[20]

Figure 6 shows an image taken at higher frame rate (1000-1500 fps) for a smaller region of interest near a single vane section for the 8V and CV cases. Both are at an O/A of 3 but use rotation speeds of 1800 RPM and 1200 RPM for the 8V and CV cases, respectively.

As noted previously, all vane types for the larger V05 contactor unit have vanes that do not extend all the way to the housing wall. As demonstrated in previous CFD simulations,[6] the addition of a vane-wall gap leads to a region of high rotating velocity near the housing wall and reduces the vanes' pumping efficiency leading to a higher overall annular liquid height. Thus, in each case there is a high velocity region just outside the vane tip. In the straight vane case, the flow impinges on the upstream side (with respect to rotor rotation) of the vane and flows radially inward with a visual appearance analogous to traditional turbulent flow over a flat plate. In the curved vane case, the flow is more efficiently directed radially inward on the upstream side; however, on the backside of the vane there is separation of the flow and an unstable stagnation region forms near the radial midpoint of the vane. As noted previously, low flow regions are characterized by darkened appearance due to dispersed phase accumulation. The general flow pattern around the curved vane is reminiscent of aerodynamic flow over a wing at high angle of attack where flow separation occurs.

ERT

A circumferential array of 32 square electrodes inset into the housing of the 12.5 cm contactor near the bottom of the rotor enables measurements of the cross-sectional

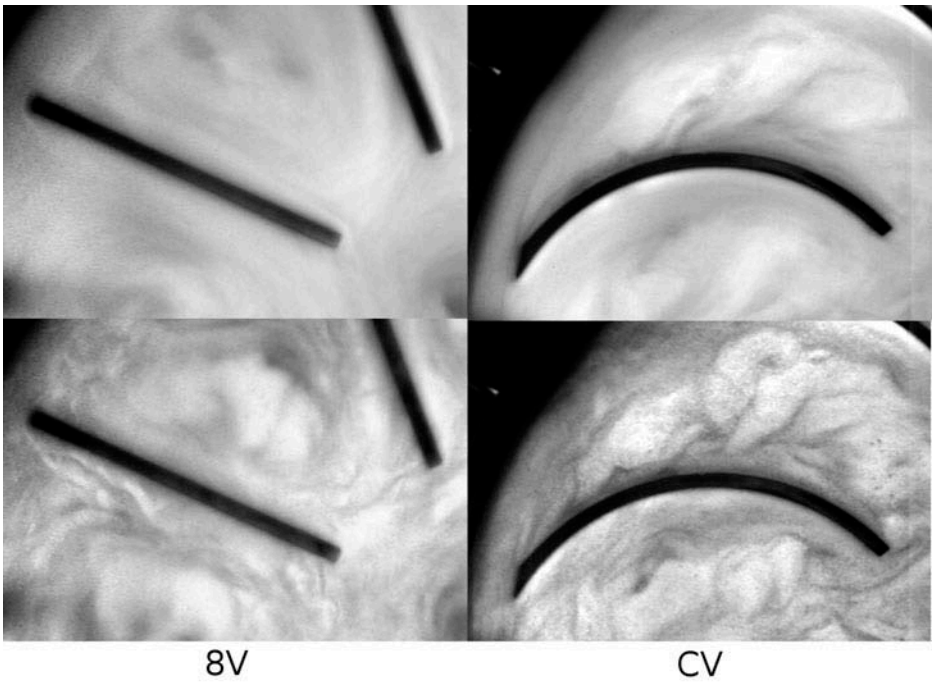

Figure 6 Zoomed-in view of flow around a single vane for the 8V and CV cases at O/A = 3 and a total flowrate of 10 LPM. Top row shows time-averages while bottom shows instantaneous snapshots. Rotor rotation is in a clockwise direction.

distribution of electrical conductivity which in turn can be related to phase fraction distribution. For the three-phase case of liquid–liquid–air, the quantitative interpretation of the data becomes problematic given that both the organic phase and air have essentially zero conductivity. However, it is possible to compare the results quantitatively in relative terms for cases with different vanes at the same conditions. As noted in the description of the experimental setup, measurements were initially done using the aluminum nitrate nitric acid solution and 40% TBP in dodecane. As discussed earlier, there were limitations on injection current of the ERT system due to the high conductivity of the aqueous phase in that liquid–liquid pair. It was also found that a consistent asymmetric non-uniformity was observed in the few acceptable measurements that were made for each case. In typical ERT setups such as in a stirred tank, only a single grounding electrode is usually required. However, in the centrifugal contactor, where electric field lines are more geometrically constrained, it was found that four linked ground electrodes equally spaced around the ring was required. With this modification and switching to the 0.01 M nitric acid and 30%TBP in dodecane phase pair, successful measurements were achieved. Only measurements comparing the 4V and CV geometries were performed. Reconstruction of the voltage measurements was done using the SCGImage software from Industrial Tomography Systems (ITS) which uses the sensitivity conjugate gradient method[21] for reconstruction of the tomographic data from pairwise voltage measurement data from the ERT sensor. It was previously found that given the internal restrictions of the rotor and vanes, explicit inclusion of the non-conductive "void" geometry of the contactor housing vanes into the finite element mesh

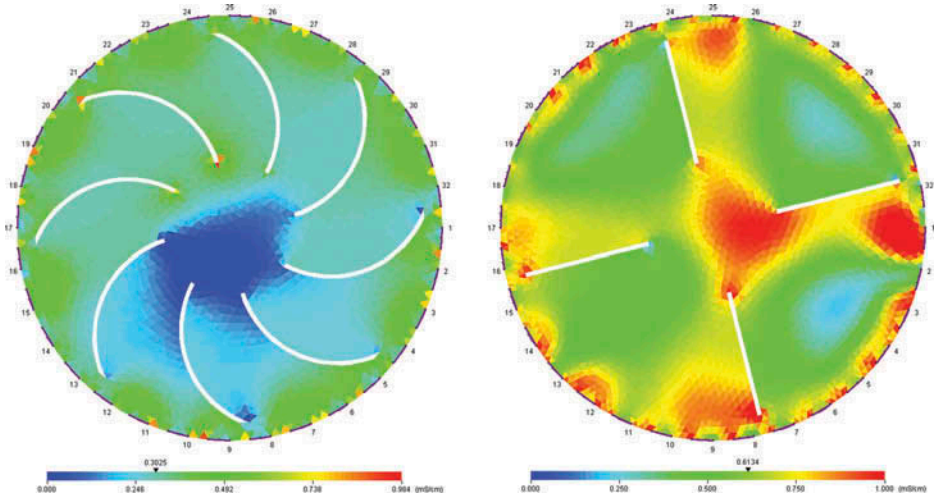

Figure 7 Comparison of reconstructions for CV (left) and 4V (right) configurations using meshes with explicit vane geometry. Data are averaged over 10 measurement frames (∼2 seconds).

of the measurement plane significantly improved the quality of the reconstruction.[12] Only simple circular mesh options are available in the SCGImage software by default. With input from ITS and their university partners in regard to mesh requirements and format, custom finite element mesh files for the centrifugal contactor geometry, including explicit mixing vane structures were successfully generated using the CUBIT software (http://cubit.sandia.gov) and converted to the format required by the SCG software. A set of measurements was made for liquid–liquid operation at an approximate O:A phase ratio of 1:3 and a total flow rate near 10 L/min with a rotor speed of 1800 RPM. Identical test conditions were used for both the CV and 4V geometries and reconstructions of the conductivity map—taking the aqueous phase condition as the reference measurement—are shown in Fig. 7.

These results show that the volume fraction occupied by the electrically conductive phase (aqueous)—which is obtained by taking the temporo-spatial average of the concentration map—is only 0.30 in the CV case as compared to 0.61 in the 4V case. Data shown are averaged across 10 measurement frames—which at an acquisition rate of approximately 5 Hz covers a time period of ∼2 seconds. An O:A phase ratio of 1:3 is equivalent to an aqueous phase fraction of 0.75. For reference purposes, if one assumes that the overall phase fraction on the measurement plane should be close to the feed phase ratio (which is not necessarily the case), the aqueous phase fraction decrease in both cases is accounted for by the excess fraction of entrained of air. In the 4V case, there are sometimes large air voids that form within the rotating region in each quadrant that can be observed visually through the transparent vane plate since these voids often extend to the bottom of the housing. These voids are evident in the ERT reconstructions; however, since their formation, location, and size are not fixed in time, but can be somewhat periodic and exhibit a precessing axis of rotation within the intra-vane region, the resulting time-averaged data is more diffuse than any of the individual data frames.

In the CV case, there are no stable, large-scale voids seen at the bottom of the housing. However, the ERT reconstruction shows a region of near-zero conductivity (air or organic) near the center position. While no direct measurement is available to confirm if this is

a real condition or simply an artifact of inaccurate 2D reconstructions of the ERT data due to the challenging configuration and restricted geometry of the centrifugal contactor, this result is qualitatively confirmed by visual observation of the cloudiness of the dispersion in the lower portion of the mixing region (see Fig. 4, top row). Additionally, the amount of entrained air from the mixing zone being pumped into the rotor is greater for the CV case given that the overall liquid height is much lower and the vanes are designed to efficiently direct flow into the rotor. Experimentally, this more significant pumping of air can qualitatively be confirmed by "feeling" the outflow of air from a vertical vent pipe in the light phase outlet—in fact, the vent on the outlet line is recommended on account of this air pumping and to avoid excess foam formation. Furthermore, previous CFD simulations comparing flow with different mixing vanes in centrifugal contactors has also shown greater entrainment and air pumping in the CV configuration.[6] An alternate explanation of this region of low conductivity in the CV case is that it is a stable isolated region of organic continuous dispersion rather than a pocket of air. This could be the case if incoming organic phase is able to bypass the annular space without significant mixing and get quickly beneath the rotor. For reference, the organic inlet is positioned above electrodes 11-12-13. Identification of disparate continuous phase between the annular space and the mixing vane region in centrifugal contactors has been noted in some studies. Additional measurements would be needed to determine if this is the case here.

Droplet Size Distribution

Quantitative direct comparison of the dispersed phase droplet size in the mixing zone for different mixing vane configurations offers a definitive evaluation of the impact of mixing intensity and liquid height differences observed through qualitative high-speed imaging. While a variety of measurement techniques are possible, as noted previously *in situ* imaging is used here as it has been shown to be the most consistent. That said, the number of measurements that can be performed becomes somewhat limited given the time-consuming step of image processing to identify and size droplets.

Consideration was given to the selection of the measurement location as it is important to provide the best spot to give a reliable comparison between different vane types. The potential limitations of the work of Wyatt et al.[14] in this regard were noted earlier. Rather than taking images at the side of the rotor, the droplet size was evaluated beneath the rotor through the clear housing vane plate of the 12.5 cm contactor. The flatness of this surface also avoids any issues with compensating for the curvature of the housing wall when imaging through the side. Initially, there was a slight spatial restriction with the setup which limited the reach of the camera to the periphery of the base. Consequently, the initial set of data included multiple points in the periphery of the mixing vane region for the CV configuration and a single point for the 4V (Fig. 8), both at a calibrated total flow rate of 10 L/min and an O/A ratio of 1/3 at a rotor speed of 1800 RPM. This gives the first quantitative comparison of droplet size in different housing vane configurations.

Subsequently, the setup was reconfigured to allow for measurements at the center of the vane plate to provide the most consistent location for comparison between the two vane types and avoid local variability due to proximity to the vanes or asymmetry in the geometry relative to the measurement location. One limitation that must be accepted when imaging multiphase flows through a window in this way is that while the use of an intrusive probe is avoided, only the drops in the layer close to the wall are observed.

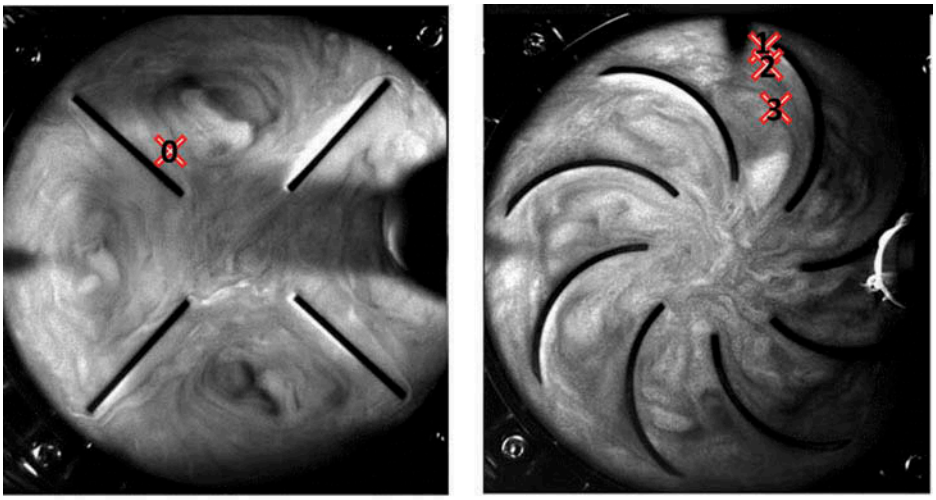

Figure 8 Approximate locations of measurements for (a) 4V and (b) CV configurations. Note, the flow in the image is an example only and not the conditions of the actual measurement.

Five to ten images of sufficient quality for semi-manual analysis of droplet size distributions were obtained at each point. More than 1000 droplets were identified in each case. While promising automated image processing tools are reported in the literature,[22] such tools require ideal backlit conditions giving good contrast to be effective. Backlighting was not possible in this case and the optimum contrast was found when positioning the strobe light at a relatively shallow angle. Image analysis was done manually with the aid of the ImageJ software package (http://rsbweb.nih.gov/ij/) which assists the user by marking, measuring, and logging each manually-identified bubble/droplet. Figure 9 gives an example image set (pre- and post-processing) for a point 1.4 mm radially inward from the vane tip of one of the curved stationary housing vanes (point (1) in Fig. 8b).

The measured distributions for the two vane configurations as taken at the several locations in Fig. 8 are shown in Fig. 10 and those obtained at the center position (rotor axis) of the housing bottom plate are shown in Fig. 11.

The distributions are characterized by the Sauter mean diameter d_{32} and the volume mean diameter d_{30}. The corresponding mean diameter data are summarized in Table 1.

From the first set of measurements, it is not possible to make a definite conclusion regarding the relative droplet size found in the two geometries though it is clear they are each in the same range with significant overlap in the distributions. Additionally, both also have a typical log-normal shape. The subsequent measurements at the center position give a more clear comparison of the relative droplet size in the two configurations. It is observed that the distribution as characterized by the value of the Sauter mean diameter d_{32} at this location is 27% smaller in the case of 4V (58.5 μm) as compared to CV (80.6 μm). As the specific interfacial area increases with the inverse square of the diameter d_{32}, this translates to a nearly 38% increase in liquid–liquid specific interfacial area at the droplet level. It can also be seen that the distributions at points in the CV geometry are somewhat broader than those in the 4V case. This is indicative of more thorough mixing on account of the greater liquid height and longer residence time of the fluid in the 4V geometry. Given that only

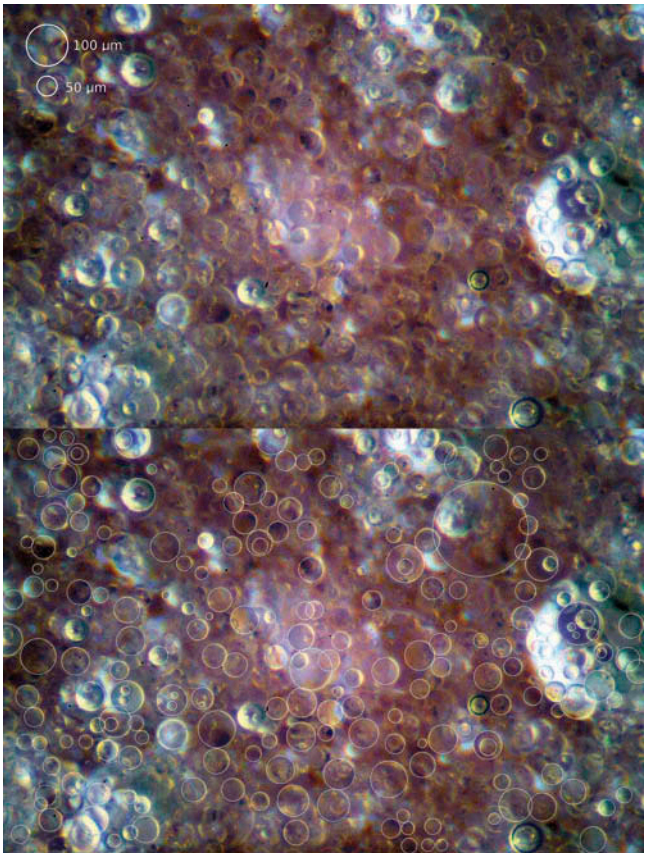

Figure 9 Example images of organic droplets (and air bubbles). The original image (normalized) is shown at the top and the processed image with marked circles at the bottom.

the drops near the housing bottom are possible to observe and measure with this configuration, additional measurements using probe based techniques or insight from multiphase CFD studies will be necessary to explore the droplet size near the rotor surface—where the turbulence intensity is at its greatest and the droplet size can reasonably be expected to be at its smallest.

These data show significantly smaller values for the droplet size than those reported in the lab-scale CINC V02 with water/PDMS at 300 mL/min ($d30 = 165$ μm at 3000 RPM) as reported by Wyatt et al.[14] This is to be expected as the viscosity of PDMS is greater than that of TBP/dodecane by about a factor of 2. Further, one would expect improved operation leading to smaller droplet sizes at what is a mid-range throughput in the V05 (approximately 50% of max throughput) as compared to the low flow conditions (only ~16% of the max) used in the case of the Wyatt et al. data for the V02. For the present case, the liquid height was approximately 4-6 cm above the rotor bottom in the CV case and ~10-12 cm in the 4V (see Fig. 4 top row). In addition, even for the same liquid phases and conditions, it should be expected that a time averaged measurement of droplet size on the side such as done by Wyatt et al. would give a different—most likely much larger—value compared to the bottom of the housing where more mixing has occurred "upstream"

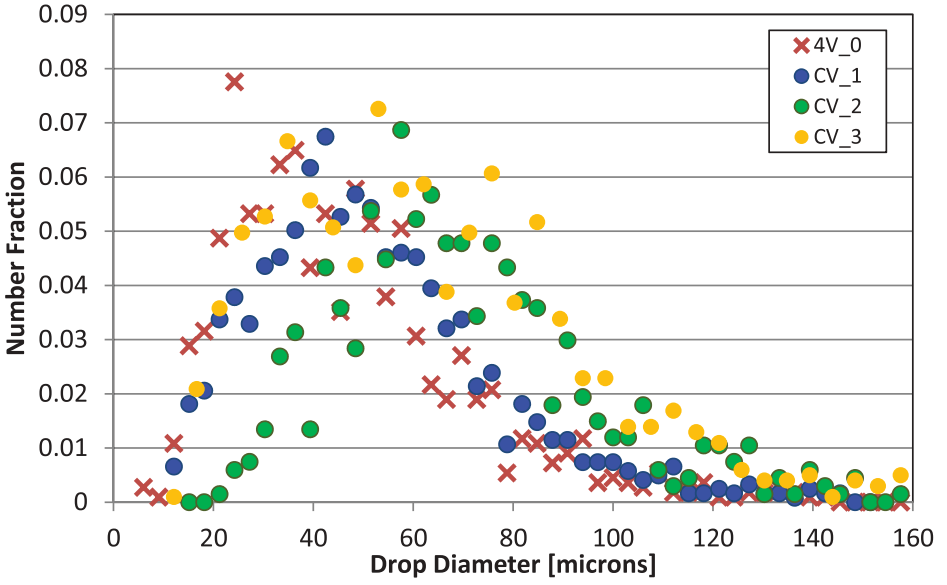

Figure 10 Droplet size distributions (in microns) for the locations shown in Figure 8 for the 4V and CV geometries at identical flow conditions: 10 L/min, O/A 1/3 and 1800 RPM.

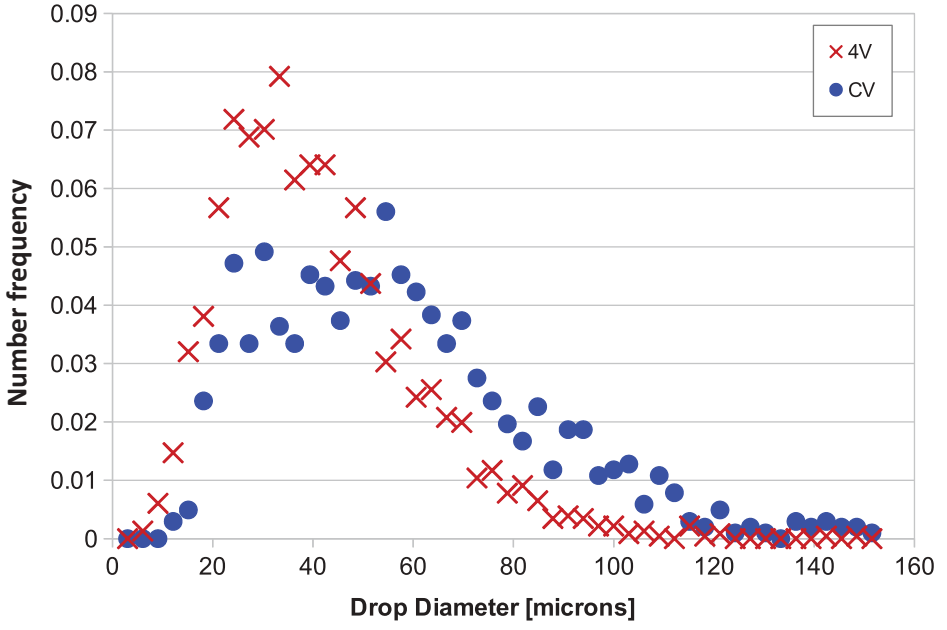

Figure 11 Droplet diameter distributions at the center position for the 4V and CV geometries at identical flow conditions: 10 L/min, O/A 1/3, and 1800 RPM.

Table 1 Summary of mean droplet sizes (d_{32} and d_{30}) for the various locations labeled in Figure 8 along with those at the center position.

Location	d_{32} [μm]	d_{30} [μm]
$4V_0$	74.8	62.8
$4V_{Center}$	58.5	49.1
CV_1	74.7	59.3
CV_2	101.5	85.3
CV_3	106.8	83.3
CV_{Center}	80.6	68.0

in the annular gap. Note that the values found here in this current study for the four vane and curved vane cases are also smaller than the corresponding simulation results presented in Wardle[7] which were intended to match the conditions used by Wyatt et al.

CONCLUSIONS

A number of experimental results for several different mixing vane options including 4, 6, and 8 straight vanes and 8 curved vanes are reported here for operation of a 12.5 cm engineering-scale centrifugal contactor unit. When taken in composite, this data gives a compelling case for close consideration of mixing vane geometry when evaluating hydraulic operation and extraction process efficiency of annular centrifugal contactors. While the mixing vane geometry is only one possible design alternative (e.g., annular gap size), it is one that can be optionally configured for contactor installations and in particular those which include a separate housing bottom vane plate rather than one integral to the housing body, such as those from CINC Industries.

These results suggest that when operating a process at a total throughput of less than 50% of the maximum, the use of a four straight vane configuration offers the potential for enhanced mixing and process improvement. While one typically aims to design a process operating near maximum unit capacity, there are some cases in which lower flow rates may be employed. For example, one might aim to increase hold-up volume and decrease throughput for processes which have kinetic limitations where even modest increases in mixing zone residence time and interfacial area can have a significant impact on overall performance. Additionally, if the same size contactors are used for each section in a full process implementation, it becomes impossible to operate each section near the maximum unit design throughput as the total throughput of a given stage is defined by the chemical process (i.e., specified O/A ratio in a given section and total solvent flow rate employed in the process). In such a case, the scrub and strip sections may have significantly lower throughput than the extraction section and one might choose to make a different housing vane selection there to improve performance of these stages.

For general operation over the full range of a device's throughput with a fixed vane configuration, six straight vanes may give the best balance between throughput flexibility and mixing optimization. Use of four straight vanes results in an approximately 50% decrease in the maximum throughput compared to curved mixing vanes—with the trade-off of a modest enhancement in both mixing zone residence time (i.e., greater hold-up volume) and liquid–liquid interfacial area (i.e., smaller droplet size). While presently only the hydraulic liquid–liquid operation has been explored here, extraction studies which compare the mass transfer efficiency of contactors using the different vane configurations for

processes which are sensitive to mixing and residence time (e.g., TALSPEAK[23]) would be a logical next step to further establishing the basis for vane type selection.

ACKNOWLEDGMENTS

Thanks to a number of summer students who contributed to this work including Jing Gao (University of Illinois at Chicago), John Caputo (Iowa State University), and Lucas Dunshee (Iowa State University). Thanks also to Jay Margolis of Infinity Photo-Optical and Robert Root of Prism Science Works.

FUNDING

This work was supported by the U.S. Department of Energy, Office of Nuclear Energy, under Contract DE-AC02-06CH11357.

REFERENCES

1. Bernstein, G.; Grosvenor, D.; Lenc, J.; Levitz, N. A high-capacity annular centrifugal contactor. Nucl. Technol. **1973**, *20*, 200–202.
2. Bernstein, G.; Grosvenor, D.; Lenc, J.; Levitz, N. *Development and Performance of a High-Speed Annular Centrifugal Contactor*; Technical Report ANL-7969, 1973.
3. Seader, J.; Henley, E. J. *Separation Process Principles*; Wiley: NY, 1998.
4. Leonard, R.; Pelto, R.; Ziegler, A.; Bernstein, G. Flow over circular weirs in a centrifugal field. Can. J. Chem. Eng. **1980**, *58*, 531–533.
5. Wardle, K. E.; Allen, T. R.; Anderson, M. H.; Swaney, R. E. Experimental study of the hydraulic operation of an annular centrifugal contactor with various mixing vane configurations. AICHE J. **2010**, *56*, 1960–1974.
6. Wardle, K. E.; Allen, T. R.; Anderson, M. H.; Swaney, R. E. Analysis of the effect of mixing vane geometry on the flow in an annular centrifugal contactor. AICHE J. **2009**, *55*, 2244–2259.
7. Wardle, K. E. Hybrid multiphase CFD simulation for liquid–liquid interfacial area prediction in annular centrifugal contactors. *Proceedings of Global 2013*, 2013; p 7650.
8. Birdwell, J. F.; Anderson, K. K. *Evaluation of Mass Transfer Performance for Caustic-Side Solvent Extraction of Cesium in a Convenional 5-cm Centrifugal Contactor*; Technical Report ORNL/TM-2001/278, 2002.
9. Schuur, B.; Jansma, W.; Winkelman, J. G.; Heeres, H. J. Determination of the interfacial area of a continuous integrated mixer/separator (CINC) using a chemical reaction method. Chem. Eng. Process: Process Intensification **2008**, *47*, 1484–1491.
10. Schuur, B.; Kraai, G. N.; Winkelman, J. G.; Heeres, H. J. Hydrodynamic features of centrifugal contactor separators: Experimental studies on liquid hold-up, residence time distribution, phase behavior and drop size distributions. Chem. Eng. Process: Process Intensification **2012**, *55*, 8–19.
11. Kadam, B.; Joshi, J.; Koganti, S.; Patil, R. Dispersed phase hold-up, effective interfacial area and Sauter mean drop diameter in annular centrifugal extractors. Chem. Eng. Res. Des. **2009**, *87*, 1379–1389.
12. Wardle, K. E. *Summary of Multiphase Measurements from Contactor ERT Facility FY11 Experiments*; Technical Report ANL-LTR-CERT-11-001, 2011.
13. Maaß, S.; Wollny, S.; Voigt, A.; Kraume, M. Experimental comparison of measurement techniques for drop size distributions in liquid/liquid dispersions. *Exp. Fluids* **2011**, *50*, 259–269.
14. Wyatt, N. B.; OHern, T. J.; Shelden, B. Drop-size distributions and spatial distributions in an annular centrifugal contactor. AICHE J. **2013**, *59*, 2219–2226.

15. Sathe, M.; Deshmukh, S.; Joshi, J.; Koganti, S. Computational fluid dynamics simulation and experimental investigation: Study of two-phase liquid-liquid flow in a vertical Taylor-Couette contactor. Ind. Eng. Chem. Res. **2010**, *49*, 14–28.
16. Wardle, K. E. *FY12 Summary Report on Liquid-Liquid Contactor Experiments for CFD Model Validation*; Technical Report ANL-LTR-CERT-12-002, 2012.
17. Dickin, F.; Wang, M. Electrical resistance tomography for process applications. Meas. Sci. Technol. **1996**, *7*, 247–260.
18. Padial-Collins, N. T.; Zhang, D. Z.; Zou, Q.; Ma, X. Centrifugal contactors: Separation of an aqueous and an organic stream in the rotor zone (LA-UR-05-7800). Sep. Sci. Technol. **2006**, *41*, 1001–1023.
19. Wardle, K. E.; Weller, H. G. Hybrid multiphase CFD solver for coupled dispersed/segregated flows in liquid-liquid extraction. Int. J. Chem. Eng. **2013**, *2013*, 128936.
20. Wardle, K. E.; Allen, T. R.; Swaney, R. CFD Study of the flow in an annular centrifugal contactor. Sep. Sci. Technol. **2006**, *41*, 2225–2244.
21. Wang, M. Inverse solutions for electrical impedance tomography based on conjugate gradients methods. Meas. Sci. Technol. **2002**, *13*, 101–117.
22. Maaß, S.; Rohan, J.; Hansch, R.; Kraume, M. Automated drop detection using image analysis for online particle size monitoring in multiphase systems. Comput. Chem. Eng. **2012**, *45*, 27–37.
23. Nichols, K. P.; Pompano, R. R.; Li, L.; Gelis, A. V.; Ismagilov, R. F. Toward mechanistic understanding of nuclear reprocessing chemistries by quantifying lanthanide solvent extraction kinetics via microfluidics with constant interfacial area and rapid mixing. J. Am. Chem. Soc. **2011**, *133*, 15721–5729.